ONR Arctic and Global Prediction Program: NOO O14-1 5 – 1 – 25 77: Beryllium-7 as a tracer of solar heating of the surface waters of the Arctic Ocean during the 2015 US GEOTRACES Arctic cruise
Award Amount: $78,943
Award Time Period:
9/1/2015-8/31/2017

1.0 Introduction

One of the important considerations in the summer surface energy balance of the Arctic Ocean is the fate and partitioning of the energy input (mostly shortwave radiation) in the heterogeneous ice-ocean system during the melt season. Downwelling solar radiation through leads and at the ice edge is a primary source for the direct heating of the ocean, but the fate of the solar energy absorbed through the open water is not well understood [Ingram et al., 1989; Rind et al., 1995]. It is not known for example, the extent to which this heat laterally melts the ice in contact with the leads or ice edge, is conveyed to depth and melts the ice from below, or is transported away from the ice (e.g. Maykut and Perovich, 1987; Perovich et al., 2008). The fate of the heat has direct consequence therefore upon the persistence of the ice cover and the associated summertime albedo. ***Understanding these issues is critical for improving predictions of the future state of ice cover in the Arctic.***

This study evaluates these issues (the source, timing, partitioning, and fate of heat input), using the naturally occurring radioactive tracer, ^{7}Be. The work was performed during the 2015 US Geotraces Arctic cruise (Fig 1). Beryllium-7 is a cosmic ray-produced species that is delivered to the Earth's surface and, as such, is a form of proxy for incoming solar radiation. Because of its 53.3 day half-life (77 d mean life), it is an ideal tracer of water that has been in contact with the sea surface over the past season (Kadko and Olson, 1996), and by inference, a tracer of heat and other properties deposited at the sea surface. It has already proved to be an ideal tracer for such investigations in the Arctic (Kadko, 2000; Eicken et al., 2002; Kadko and Swart, 2004).

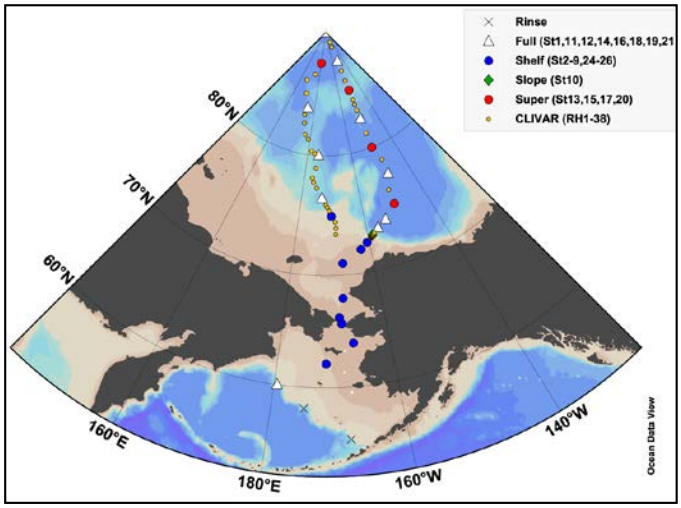

Figure 1. US Arctic GEOTRACES cruise track

^{7}Be is an independent proxy that will help answer a key question that has plagued study of the heat budget of the Beaufort Gyre for a long time: How much of the bottom and side melt, which have outweighed surface melt in recent years (Perovich et al., 2008; Steele et al, 2010), is contributed by <u>local</u> solar heating, or <u>non-locally</u> from heat advected from the Bering and Chukchi Sea?

In addition, other questions can be addressed with this tracer:

How much of incoming solar radiation is partitioned into the upper ocean versus reflected (or absorbed) by the ice? What is the partitioning of solar heat in the upper ocean between "storage" and ice-melting? What is the magnitude of vertical mixing between the upper pycnocline and the surface mixed layer? *These elements will contribute to the validation of modeling efforts aimed at assessing the future trajectory of the Arctic sea ice cover.*

While models have simulated a reduction of Arctic sea-ice, the observed decay *rate* of ice-cover over the past three decades is greater than the model estimates (Stroeve et al., 2007; Kwok and Untersteiner, 2011). This suggests the need for better understanding of oceanic processes (e.g. ice-albedo feedback, oceanic heat flux, vertical mixing) that tracer studies such as proposed here can provide.

2.0 Background

As a tracer, ^{7}Be ‘‘time-tags’’ water in contact with the ocean surface, which provides evidence of air/sea interaction during the previous seasonal period. Penetration of the characteristically high mixed layer concentrations of ^{7}Be into the upper thermocline has been used to trace ocean ventilation and subduction (of water mass, heat and chemical properties) over seasonal timescales within numerous ocean regimes (e.g. Kadko and Olson, 1996; Kadko and Johnson, 2008; Kadko, 2009) including the Arctic (Kadko, 2000; Kadko and Swart, 2004). In these works, the ^{7}Be tracer is used to 1) infer ventilation rates of water, heat, and chemical properties that had previously been near the surface within the timescale of the isotopic mean life of 77 days, 2) derive mixing rates between the mixed layer and upper thermocline and 3) in the Arctic, trace the source and fate of heat in the upper ocean-ice system. The tracer has also been used to infer upwelling rates in the Equatorial Atlantic, and ^{7}Be profiles were used to constrain vertical diffusivity within the upper thermocline (Kadko and Johns, 2011). Vertical mixing can likewise be evaluated in the Arctic.

In figure 2, a simplified schematic illustrates how in the Arctic, the atmospheric input of ^{7}Be ("X" dpm/cm^{2}) is diminished in open water ("Q") by the relative fraction of open vs. ice covered water.

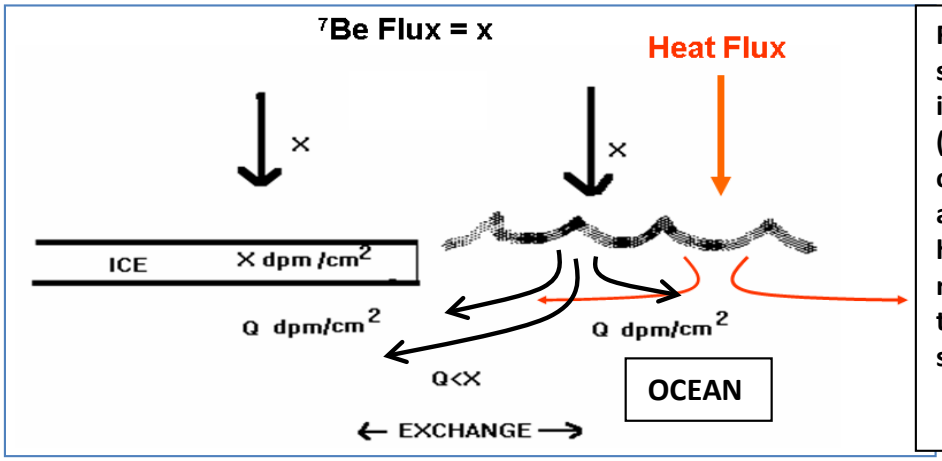

Fig 2. ^{7}Be (black arrows) serves as a proxy for incoming solar radiation (red arrows) through open water. The association of ^{7}Be with heat "tags" that heat as recently input, and serves to track its fate over a seasonal timescale.

Water, tagged with ^{7}Be (and heat), moves through the water column and under the ice. There are numerous applications of this tracer to the Arctic:

1) The [heat /^{7}Be] flux ratio, along with the inventory of ^{7}Be in the water column, provides an integrated measure of the local, solar heat input through open water during the previous months. The relative value of "Q" and "X" allows assessment of the partitioning of heat absorbed into the upper ocean.

2) The penetration of ^{7}Be to depth provides a means to derive vertical mixing rates.

3) The association of ^{7}Be with heat "tags" the heat as recently input, and serves to track its fate over a seasonal timescale.

This was shown dramatically during the SHEBA (Beaufort and Chukchi sea region) project in 1997 (Fig 3). The heat and fresh water content of the SHEBA site was much greater than that measured during AIDJEX 20 years earlier (Maykut and McPhee, 1995; McPhee et al., 1998). A warm layer (0.5^{o}C greater than the mixed layer) was observed below the mixed layer in the fall. Remnant ^{7}Be associated with this layer (red circled data) marked the warm water as having been in contact with the sea surface within the previous ~77 d. Thus the heated layer beneath the October mixed layer was remnant of an earlier, deeper, mixed layer and was the result of very active heat input in the previous late spring-summer. It was shown (Kadko, 2000; Kadko and Swart, 2004) that this heat could not have been advected from afar, and was a direct consequence of greater local heat input due to 3-fold greater open water during SHEBA as compared to AIDJEX. This heat was essentially trapped (i.e. "stored") in this layer until such time as subsequent mixing events would have made it available for future ice melt. This result was a critical piece of information for reconstructing the evolution of the heat inventory of the site, and provides a basis for modeling the source and fate of heat as open water in the Arctic increases (McPhee et al. 1998, Kadko, 2000). This is significant, as this warm layer, described as the near-surface temperature maximum (NSTM) in the Canada Basin, is at present evolving in temperature, spatial extent, and depth (Jackson et al., 2010). The partitioning of solar heat between "storage" and ice-melting likely is evolving as well, and will affect the future ice mass balance and strength of the ice albedo feedback.

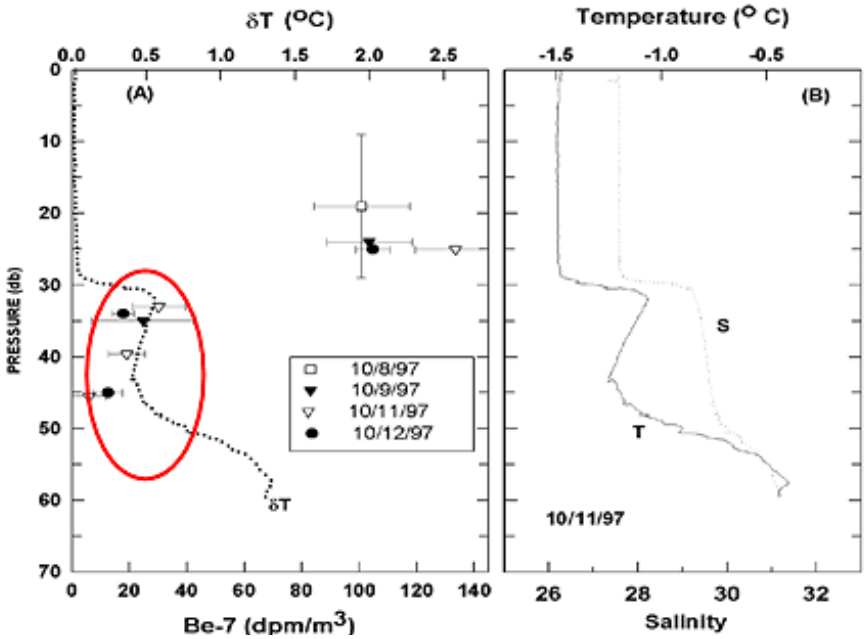

Fig 3. (A) ^{7}Be from the October 1997 occupation of the SHEBA site (symbols), displayed with the δT (temperature above freezing) profile. Remnant ^{7}Be below the mixed layer (circled in red) proved that the associated large heat inventory resulted from earlier local heat input through extensive lead coverage.

(B) Temperature and salinity profiles from the SHEBA site (Kadko, 2000)

Compelling evidence of the association of ^{7}Be with summer heating is presented in Figure 4, which shows the δT (temperature above freezing) and ^{7}Be profile through a lead in mid-July 1998. High heat and ^{7}Be were trapped in the upper fresh layer until July 18, when meltwater from the lead began to flow under the adjacent ice [Paulson and Pegau, 2001]. Reflecting this, the data show that heat and ^{7}Be in the upper lead dropped proportionately between July 15 and July 22.

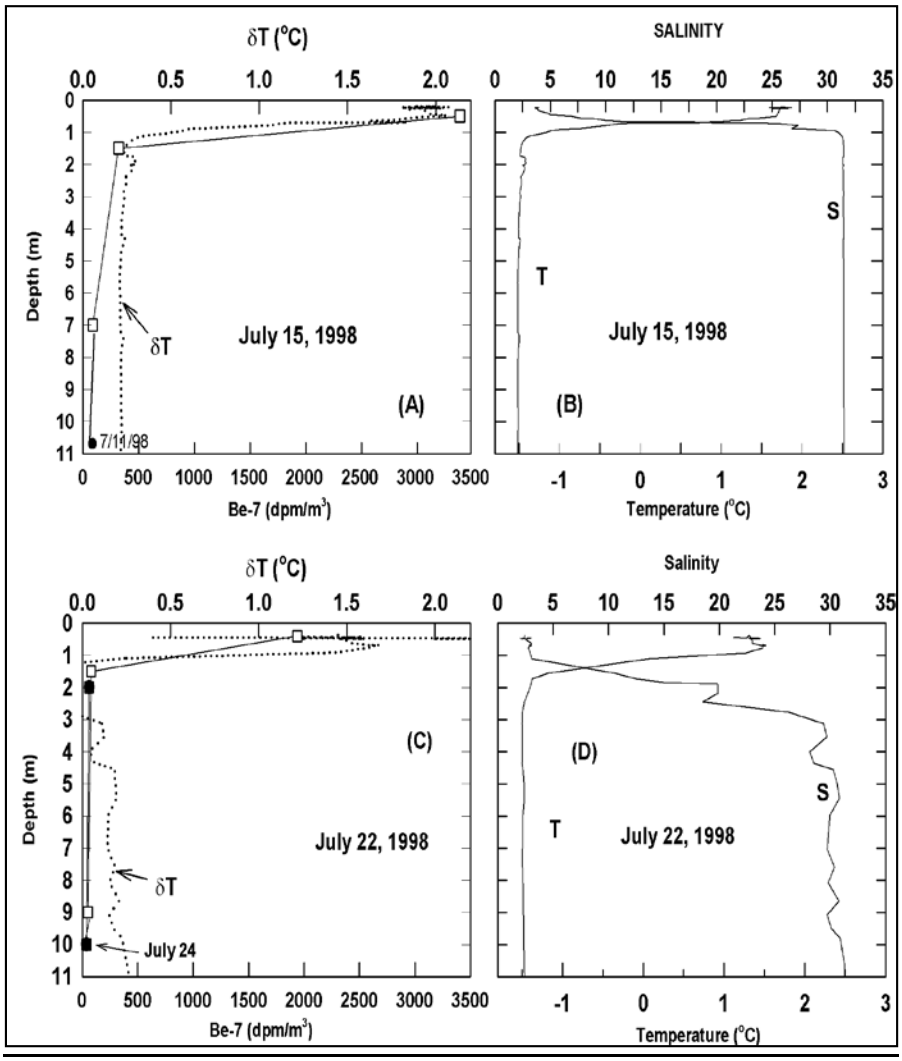

Fig 4. (a) ^{7}Be measurements (symbols) though the upper 10 m of a lead are displayed with the δT (temperature above freezing) profile of July 15, 1998. (b) Temperature and salinity profiles through the lead, July 15, 1998. (c) ^{7}Be measurements through the same lead are displayed with the δT profile of July 22, 1998. *Note the drop in ^{7}Be and heat from the earlier measurement as meltwater leaked under the adjacent ice*. (d) Temperature and salinity profiles through the lead, July 22, 1998 (Kadko and Swart, 2004).

3.0. Goals

To goal of this work is evaluate the source, timing, partitioning, and fate of heat input, and the consequent effect on the ice cover in the Chukchi and Beaufort Seas, where there have been large changes in ice conditions in recent years. The study applys measurements of the isotope ^{7}Be, which has proven to be a useful tracer of heat transport within the Arctic Ocean. These measurements were made within an extensive CTD, XCTD, and XBT survey provided by the PI and the accompanying CLIVAR component of the GEOTRACES cruise. Such CTD surveys are critical, but they can only offer description of the heat and fresh water regime; alone this is insufficient to establish a chronology and source for these distributions. The ^{7}Be tracer provides that chronology. With this information, two main contributions can be made towards understanding processes controlling upper ocean heat content and transport:

1) Determine the relative magnitudes of local and non-local processes which are driving the ice retreat, and investigate the partitioning of local solar radiation between ice melting and storage. In other words, what is the fate of the local heat input?

2) Elucidate the magnitude of vertical mixing beneath the surface mixed layer.

3.1. *Goal I - Local vs. non-local processes and the partitioning of local heat input*

An issue of active current Arctic research is the evaluation of how much of the bottom and side melt, which have outweighed surface melt in recent years (Perovich et al., 2008; Steele et al, 2010), is contributed by local solar heating, or non-locally from heat advected from the Bering Sea and Chukchi Sea (e.g. McPhee et al., 1998, Macdonald et al. 1999; Kadko, 2000; Kadko and Swart, 2004; Shimada et al., 2006; Shaw et al., 2009; Jackson et al., 2010). The isotope ^{7}Be, by the manner of its input (locally, through open water) and its short half-life (53 days), provides a tracer of local solar heating. For example, in the background section it was described how, during the SHEBA program, the association of ^{7}Be with a warm layer (below the mixed layer) in the Fall 1997 marked the warm water as having been in contact with the sea surface within the previous ~77 d. This indicated that the heated layer was remnant of an earlier, deeper, mixed layer and was the result of very active heat input in the late spring-summer. It was shown that this heat could not have been advected from afar (Kadko, 2000; Kadko and Swart, 2004). This was quantitatively assessed with a numerical model to reconstruct the evolution of the mixed layer using ^{7}Be to set the physical parameters of the model. Applying the same model parameters derived from the ^{7}Be distribution to the seasonal heat input, the observed temperature profile was also derived. The important point was that the observed ocean inventory of ^{7}Be was that expected from local input [atmospheric flux corrected for any ^{7}Be caught by the ice]. Thus measurement of ^{7}Be in the ocean, ^{7}Be in the ice, and the atmospheric ^{7}Be flux allowed us to conclude that the heat input was local and could be modeled one-dimensionally. This is consistent with Perovich et al (2008) whose calculations, based on ice mass balance, indicated that solar heating of the upper ocean was sufficient to account for the enhanced Beaufort Sea bottom melting observed a decade later. Observation of the extent of ice melt alone however cannot rule out the contribution from advective heating; as Perovich et al (2008) state: "Combining results from this [ice melt] analysis with oceanographic observations will delineate the relative contributions of local solar heating and advected ocean heat from lower latitudes". Similarly, Jackson et al. (2010) conclude that while the seasonal progression of the NSTM is dominated by the 1-D cycle of local solar heating, advective processes are important and cannot be ignored. ***This tracer work is aimed at assessing the relative contributions of local and advected sources***.

Of course, the situation at SHEBA, which suggested the dominance of local heating, is not necessarily representative across all spatial and temporal scales. What would we expect if non-local (advective) sources of heat are important? A simple, qualitative example would be the extreme case where all the heat was advective (non-local), in which case the ocean ^{7}Be inventory would approach zero. More formally, the partitioning of the upper ocean heat content between local and advective sources can be quantitatively assessed by considering the local solar heat flux and the local ^{7}Be flux to the surface ocean:

The solar heat input directly to the upper ocean (F_{rw}) can be estimated by:

$$F_{rw} = F_r(1 - \alpha_w)A_w \qquad \text{eqn. (1)}$$

where F_r is the incident solar irradiance, α_w is the albedo of the ocean, and A_w is the fractional area of ice-free ocean. This relationship represents a lower bound on the solar heat input to the upper ocean, as it does not consider the contribution from sunlight penetrating through the ice cover into the ocean (Perovich et al., 2008). Transmittance of light through bare-ice dominated areas is only ~ 5% of incident radiation, and thus is not significant, but under ponded ice could be as high as ~40% immediately beneath (~1m) the ice (Frey et al., 2011), dropping to <5% by 20 m depth.

The local flux of ^{7}Be to the surface ocean is:

$$F_{7Be} = F_a\ A_w \qquad \text{eqn. (2)}$$

where F_a is the atmospheric flux of ^{7}Be. This relationship represents a lower bound on the ^{7}Be input to the upper ocean, as it neglects ^{7}Be input to the ocean from melting snow/ice. This is readily corrected by measurements of the ^{7}Be inventory of the snow-ice-melt pond system (Kadko and Swart, 2004; Eiken et al, 2002).

Due to the radioactive nature of the ^{7}Be tracer, the expected cumulative ^{7}Be content of the water column at any time is:

$$\frac{F_{7Be}}{\lambda}(1-e^{-\lambda T}) = \Sigma^{7}Be \qquad \text{eqn. (2a)}$$

where λ is the radio-decay constant. Then, by measuring the ocean inventory of ^{7}Be, ($\Sigma^{7}Be$), the heat content of the upper ocean supplied by *local solar heating only* can be given by the expected ratio of the heat and ^{7}Be fluxes multiplied by the observed ^{7}Be inventory:

$$F_{rw}(T) = \left(\frac{F_{rw}}{F_{7Be}}\right) \times \Sigma^{7}Be \qquad \text{eqn. (3)}$$

where T is any integrative time period of interest.

In this manner, the measured (total) upper ocean heat content can be partitioned into contributions from local and advective sources as illustrated during the SHEBA experiment (Kadko and Swart, 2004). These quantities can then be compared to the heat required to produce observed bottom melting (e.g. Perovich et al., 2008). Furthermore, as described above, the association of ^{7}Be with heat "tags" the heat as recently input, and serves to track its fate over a seasonal timescale. ***This will therefore enable us to further partition the local solar heat input between "storage" and ice-melting.***

3.2 ***Goal II - Vertical Mixing:***

The ^{7}Be profiles collected for goal I above (***Local vs. non-local processes***) can be applied to model vertical mixing.

The distribution of ^{7}Be below the mixed layer can be used to evaluate the magnitude of vertical mixing in the upper pycnocline. Basically, the amount of ^{7}Be found in the "tail" layer below the mixed layer provides information on the strength of the local vertical mixing. The ^{7}Be concentration in the "tail" layer is governed to first approximation by the one - dimensional vertical advection-diffusion equation:

$$\delta C/\delta t = \frac{\partial}{\partial z}(K_z \frac{\partial C}{\partial z}) - \lambda C \qquad \text{eqn (4)}$$

where C is the concentration of ^{7}Be and K_z is the vertical diffusivity. This was used to evaluate vertical mixing at the SHEBA site, within the near-surface temperature maximum (NSTM) in October, 1997. These results suggest that in the highly stratified water below the mixed layer (see salinity gradient in Figure 2), vertical mixing was not much greater than 10^{-6} m^2s^{-1}. This layer is the most stratified part of the water column (see Brunt – Väisälä frequency analysis in Jackson et al., 2010). The effect of different pycnocline K_z on the model results is shown in Figure 5. Profiles of ^{7}Be are quite sensitive to the K_z, as higher values of K_z would draw more ^{7}Be from the mixed layer into the pycnocline water (Fig 5).

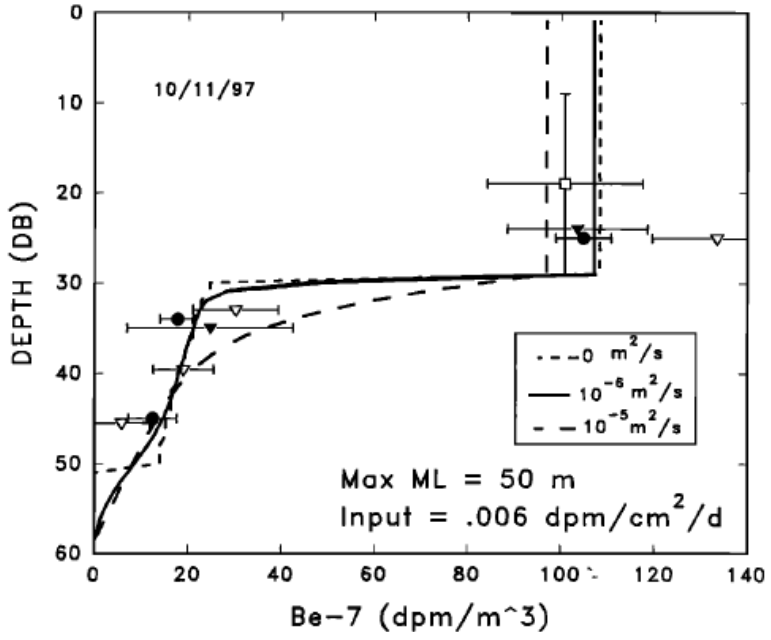

s

Figure 5. The model output for the ^{7}Be profile from the SHEBA site in Oct 1997 for three different values of Kz in the pycnocline: 0, 10^{-6}, and 10^{-5} m^2 s^{-1} (Kadko, 2000).

The PI has applied this to other areas as well, including the Bermuda Times-Series location. An example (Figure 6) is shown where a value of 7.8 x 10^{-6} m^2s^{-1} was derived for K_z from a profile collected in July, 2007. This is compared to a modeled profile in which K_z =0 is assigned.

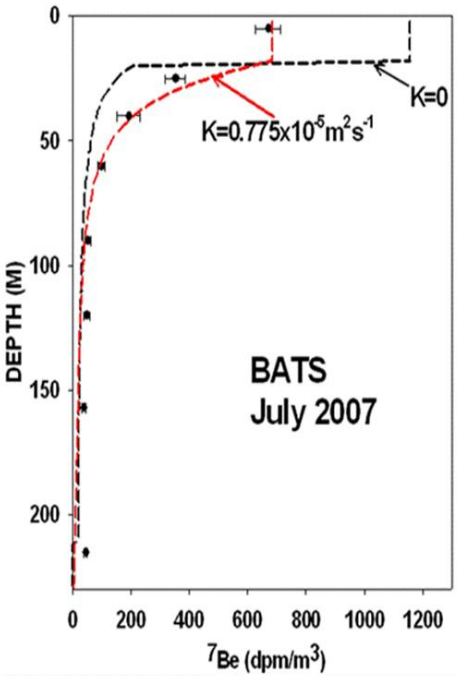

Figure 6. The model output for the ^{7}Be profile from the BATS site in July 2007.
A value of K_z in the pycnocline of 7.8x 10^{-6} m^2 s^{-1} provides a good fit to the data.
For comparison, the modeled profile with K_z=0 is shown.

Finally, this technique was applied to an upwelling region in the eastern equatorial Atlantic. Shown in figure 7 are three stations collected along the equator with the ^{7}Be profiles modeled by the one-dimensional vertical advection-diffusion equation including upwelling. In this case, the shape of the ^{7}Be profile below the mixed layer represents a competition between the upwelling, which brings deep, ^{7}Be-"dead" water toward the surface, and downward turbulent mixing of high ^{7}Be concentrations from the surface layer. The required value of K_z is derived for each profile. Also shown are the modeled ^{7}Be profiles if K_z values of a factor of two greater or smaller are used (Kadko and Johns, 2011).

It is seen that the ^{7}Be profiles are quite sensitive to the K_z values and provide a strong constraint on the magnitude of the local vertical mixing. The model results (1 - 4 x 10^{-4} m^2/s) were consistent with the K_z values determined independently from energy dissipation rate measurements from the same general area as our study (Rhein et al., 2010). Tracer-derived results may be viewed as an integrated measure of mixing events over the inherent timescale of the tracer, and as such provide a valuable comparison to the more instantaneous results derived from energy dissipation rate observations.

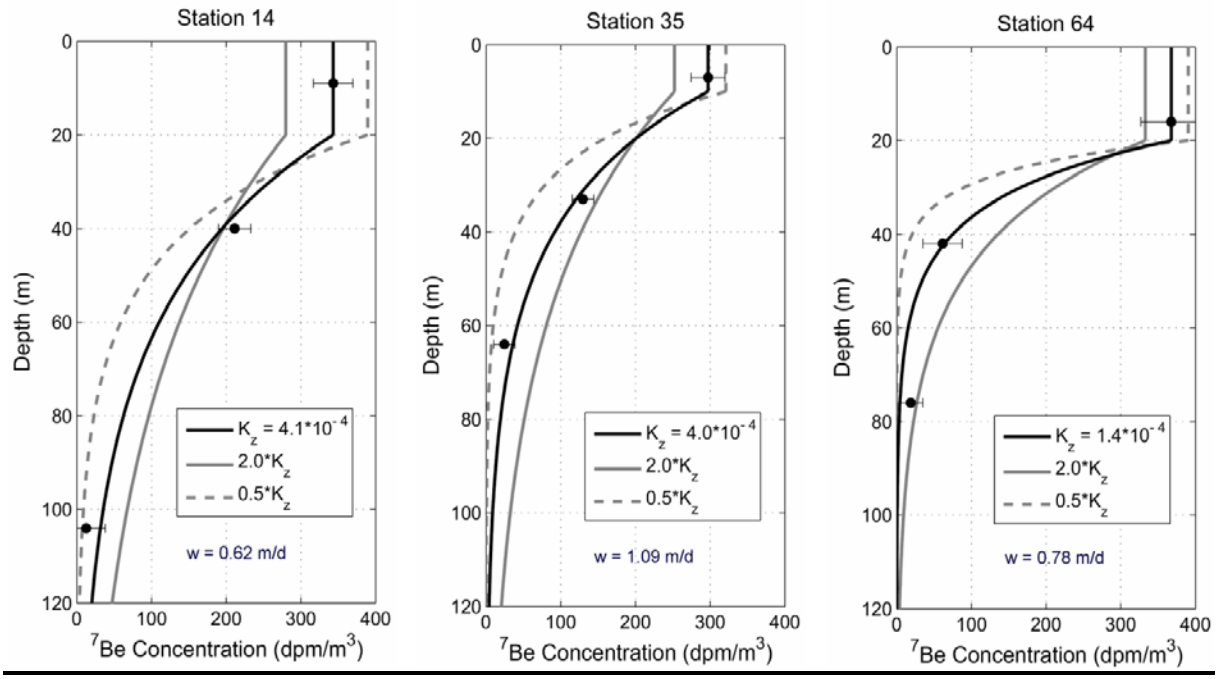

Fig. 7. ^{7}Be profiles at the stations taken along the eastern equatorial Atlantic (Kadko and Johns, 2011). The data below the mixed layer have been modeled by the one-dimensional vertical advection-diffusion equation taking into account upwelling. The required value of K_z is derived for each profile (solid line). Also shown are the modeled ^{7}Be profiles if K_z values of a factor of two greater or smaller are used. Our results (1 - 4 x 10^{-4} m^2/s) were consistent with the K_z values determined independently from energy dissipation rate measurements from the same general area as our study (Rhein et al., 2010). *The ^{7}Be profiles are quite sensitive to the K_z values and provide a strong constraint on the magnitude of the local vertical mixing.*

4.0 Methods

Seawater ^{7}Be samples: Analysis follows procedures originally developed from earlier ONR support (the SUBDUCTION experiment 1991-1992) and described elsewhere [e.g. Kadko and Olson, 1996]. Briefly, ^{7}Be is collected at selected depths by pumping seawater via a hose through iron-impregnated acrylic fibers. The hose end is attached to either a portable or ship-board CTD system. The sampling procedure has flexibility to allow sampling from a variety of platforms: ship-based sampling, collection through a hydrohole on ice, or sampling from a small boat. For ice and small boat sampling we utilize a gas-powered generator for our pumping; this has proven to be quite effective as was demonstrated during the SHEBA project (e.g. Kadko, 2000). By any sampling mode, we can routinely collect well-resolved ^{7}Be profiles (Figures 3-7) in the upper ocean.

The efficiency of the fiber for extraction of Be from seawater has been determined by adding stable (non-radioactive) Be atomic absorption standards to a drum containing seawater. The seawater was pumped through an iron fiber cartridge and the Be content of the cartridge effluent was measured by atomic absorption. From this data, integrated Be extraction efficiencies were derived.

On land, the fibers are dried, ashed, pressed into a pellet (5.8 cm diameter) and subsequently placed on a low background germanium gamma detector. The detector has been calibrated for the pellet geometry by adding a commercially prepared mixed solution of known gamma activities to an ashed fiber, pressing the ash into a pellet, and counting the activities to derive a calibration curve. The uncertainty of the extraction efficiency (4%) and the detector efficiency (2%) is smaller than the statistical counting error and the uncertainty in the blank.

Atmospheric ^{7}Be flux: The flux of ^{7}Be will be determined two ways. In one, atmospheric aerosol samples are collected through high volume air-filtration systems. The filters are counted by gamma spectrometry as described above. The aerosol ^{7}Be concentration is converted to flux by the use of commonly accepted depositional parameters (e.g. Kadko and Prospero, 2011). In addition, bulk collectors were deployed on the ship, and the collected material (both dry and wet deposition) were taken up by dilute HCl in the presence of a stable Be spike, and the ^{7}Be precipitated with iron-hydroxide, and subsequently counted by gamma spectrometry. The stable Be in the precipitate was then measured by atomic absorption to calculate the ^{7}Be recovery during precipitation (Kadko, 2000; Kadko and Prospero, 2011).

Snow and ice ^{7}Be: Snow and ice samples were also collected. These were melted, and 0.5 mL of concentrated HCl and stable Be yield tracer added (Kadko, 2000). The ^{7}Be was removed by coprecipitation with iron hydroxide, dried, and counted by gamma spectrometry as described above. The stable Be in the precipitate was then measured by atomic absorption to calculate the ^{7}Be recovery during precipitation.

5.0 Summary

There remains considerable uncertainty in high-latitude heat budget calculations because parameters such as albedo, heat transmittance through melt ponds and ice, turbulent heat flux, and cloud effects have spatial and temporal variability or are presently not well characterized. *It is for this reason that tracers, such as ^{7}Be, with relatively less complex input functions, are valuable for tagging water masses and associated heat.* Tracer studies such as this will improve our understanding of oceanic processes required for modeling efforts aimed at assessing the future trajectory of the Arctic sea ice cover.

This work contributes to investigation of the following scientific questions:

- What are the relative magnitudes of local and non-local processes which are driving ice retreat? What role does local solar radiation play in the retreat of the ice cover? How is local solar radiation partitioned between ice melting and storage?
- What is the magnitude of vertical mixing? As the ice cover retreats, do vertical mixing and upwelling of warm water in the water column occur?

References

Eicken H., R. Krouse, D. Kadko, and D. Perovich (2002) Tracer studies of pathways and rates of meltwater transport through Arctic summer sea ice. J. Geophys. Res. 107, 10.1029/200JC000583.

Frey K.E., D.K. Perovich, and B. Light (2011). The spatial distribution of solar radiation under a melting Arctic sea ice cover. Geophys. Res. Lett. 38, L22501.

Galfond B., D. Kadko, and W. Landing (in prep) A novel method of determining atmospheric deposition of trace elements to the Arctic. J. Geophys. Res

Ingram, W. J., C. A. Wilson, and J. F. B. Mitchell (1989) Modeling climate change: An assessment of sea ice and surface albedo feedbacks. J. Geophys. Res., 94, 8609-8622.

Jackson JM, Carmack EC, McLaughlin FA, Allen, S.E. and R. G. Ingram (2010) Identification, characterization, and change of the near-surface temperature maximum in the Canada Basin, 1993–2008. J. Geophys. Res, VOL. 115, C05021, 16 PP., doi:10.1029/2009JC005265.

Kadko, D. and D. Olson (1996) Be-7 as a tracer of surface water subduction and mixed layer history. Deep Sea Res. 43, 89-116.

Kadko D. (2000) Modeling the Evolution of the Arctic Mixed Layer during the Fall 1997 SHEBA Project using measurements of ^{7}Be. J. Geophys. Res, 105, 3369-3378.

Kadko D. and P. Swart (2004) The source of the high heat and freshwater content of the upper ocean at the SHEBA site in the Beaufort Sea in 1997. J. Geophys. Res. 109, C01022, doi:10.1029/2002JC001734

Kadko, D. and R. Johnson (2008) Insights into 18 degree mode water formation from measurements of ^{7}Be at the Bermuda Time-Series station. Ocean Sci. Meet. Suppl., Abstract.

Kadko, D. (2009) Rapid oxygen utilization in the ocean twilight zone assessed with the cosmogenic isotope ^{7}Be, Global Biogeochem. Cycles, 23, GB4010, doi:10.1029/2009GB003510.

Kadko, D., and J. Prospero (2011), Deposition of ^{7}Be to Bermuda and the regional ocean: Environmental factors affecting estimates of atmospheric flux to the ocean, J. Geophys. Res., 116, C02013, doi:10.1029/2010JC006629.

Kadko, D., Johns, W. (2011) Inferring upwelling rates in the equatorial Atlantic using ^{7}Be measurements in the upper ocean. Deep-Sea Res. I,doi:10.1016/j.dsr.2011.03.004.

Kwok and Untersteiner (2011) The thinning of Arctic sea ice. Physics Today, 64 (4), 36-41.

Macdonald, R. W., E. C. Carmack, F. A. McLaughlin, K. K. Kalkner, and J. H. Swift (1999), Connections among ice, runoff and atmospheric forcing in the Beaufort Gyre, Geophys. Res. Lett., 26, 2223– 2226.

Maykut, G. A., and D. K. Perovich (1987)The Role of Shortwave Radiation in the Summer Decay of a Sea Ice Cover. J. Geophys. Res. 92, NO. C7, 7032-7044.

Maykut, G. A., and M. G. McPhee (1995) Solar heating of the Arctic mixed layer, J . Geophys. Res., 100, 24, 691-703.

McPhee, M. G., T. P. Stanton, J. H. Morison and D. G. Martinson, Freshening of the upper ocean in the central Arctic: Is perennial sea-ice melting? Geophys. Res. L ett., 25, 1729-1732, 1998.

Paulson, C. A., and W. S. Pegau (2001), The summertime thermohaline evolution of an Arctic lead: Heat budget of the surface layer, paper presented at Sixth Conference on Polar Meteorology and Oceanography, Am. Meteorol. Soc., San Diego, Calif., 14– 18 May.

Perovich, D.K., J.A. Richter-Menge, K.F. Jones, and B. Light (2008) Sunlight, water, and ice: Extreme Arctic sea ice melt during the summer of 2007. Geophy. Res. Lett. 35, L11501, 4 PP., doi:10.1029/2008GL034007

Rhein, M., Dengler, M., Sultenfuß, J., Hummels, R., H¨ uttl-Kabus, S., Bourles, B., 2010. Upwelling and associated heat flux in the equatorial Atlantic inferred from helium isotope disequilibrium. J. Geophys. Res. 115, C08021 10.1029/2009C005772

Rind, D., R. Healy, C. Parkinson, and D. Martinson (1995), The role of sea-icei n 2 x CO2 climate model sensitivity P art 1, The total influence of sea ice thickness and extent. J. Clim. 8, 449-463.

Shaw, W.J., T. P. Stanton, M. G. McPhee, J. H. Morison, and D. G. Martinson (2009) Role of the upper ocean in the energy budget of Arctic sea ice during SHEBA. J. Geophys. Res, 114, C06012, doi:10.1029/2008JC004991,

Shimada, K., T. Kamoshida, M. Itoh, S. Nishino, E. Carmack, F. McLaughlin, S. Zimmerman, and A. Proshutinsky (2006), Pacific Ocean inflow: Influence on catastrophic reduction of sea ice cover in the Arctic Ocean, Geophys. Res. Lett., 33, L08605, doi:10.1029/2005GL025624.

Steele, M., J. Zhang, and W. Ermold (2010), Mechanisms of summertime upper Arctic Ocean warming and the effect on sea ice melt, J. Geophys. Res., 115, C11004, doi:10.1029/ 2009 JC005849.

Stroeve J., M.M. Holland, W. Meier, T. Scambos and M. Serreze (2007) Arctic sea ice decline: Faster than forecast. Geophy. Res. Lett. 34, L09501, doi: 10.1029/2007GL029703.